Synthetic, Spectroscopic, and Electrochemical Studies of the Isomerically-Rich $[M(CO)_2(P_2P')X]^{+/0}$ (M = Mn, Re; X = Cl, Br; P_2P' = η^3-$Ph_2P(CH_2)_2P(Ph)(CH_2)_2PPh_2$) System: Structural Characterization of a Novel Pair of Diastereoisomers of *cis,mer*-$Re(CO)_2(P_2P')Cl$

Alan M. Bond,*[,1,2] Ray Colton,[1,2] Robert W. Gable,[3] Maureen F. Mackay,[1] and Jacky N. Walter[1]

School of Chemistry, La Trobe University, Bundoora, Victoria 3083, Australia, and School of Chemistry, University of Melbourne, Parkville, Victoria 3052, Australia

Received October 25, 1996[⊗]

Reaction of $Mn(CO)_5X$ (X = Cl, Br) with $Ph_2P(CH_2)_2P(Ph)(CH_2)_2PPh_2$ (P_2P') in refluxing xylene led to the formation of isomerically pure *cis,mer*-$Mn(CO)_2(\eta^3\text{-}P_2P')X$. Cyclic voltammograms in dichloromethane (0.1 M Bu_4NPF_6) show a reversible one-electron oxidation (process 1, $E_{1/2} = 0.142$ V) to give *cis,mer*-$[Mn(CO)_2(P_2P')X]^+$. However, in acetone (0.1 M Bu_4NPF_6) at room temperature, process 1 is not reversible and an additional redox process 4 ($E_{1/2} = 0.048$ V) is observed. Process 4 is not observed at low temperatures, and at higher temperatures in acetone it merges with process 1 and also a new reversible redox couple (process 5, $E_{1/2} = -0.411$ V) appears. A combination of electrolyses, chemical oxidation, and subsequent reduction, coupled with IR and ^{31}P NMR spectroscopies and electrospray mass spectrometry (ESMS), is used to show that processes 1, 4, and 5 are all associated with redox and interconversion reactions of different isomers of $Mn(CO)_2(P_2P')X$ and $[Mn(CO)_2(P_2P')X]^+$. Other irreversible processes due to oxidation of the different isomers of $[Mn(CO)_2(P_2P')X]^+$ are observed at very positive potentials. Reaction between $Re(CO)_5X$ and P_2P' in refluxing mesitylene gives a soluble product and a small amount of precipitate. The major soluble product was identified as *cis,mer*-$Re(CO)_2(P_2P')X$, and the oxidative chemistry is similar to that of the manganese analogues. The precipitate consists of five compounds, one of which was *cis,mer*-$Re(CO)_2(P_2P')X$. The new compounds **A**−**D** were identified as follows: **A** is *cis,mer*-$\{Re(CO)_2(P_2P')X\}_2$, a dimeric species with bridging P_2P' ligands. The spectroscopic data for **B** indicated that it was a form of *cis,mer*-$Re(CO)_2(P_2P')X$, but not the same as the major product. Compound **C** is *cis,fac*-$Re(CO)_2(P_2P')X$, and compound **D** was shown to be *fac*-$[Re(CO)_3(P_2P')]X$. The crystal structures of *cis,mer*-$Re(CO)_2(P_2P')Cl$(I) and *cis,mer*-$Re(CO)_2(P_2P')Cl$(II) show the compounds to be diastereoisomers with the same *mer* geometry of the P_2P' ligand, which of necessity generates a cavity formed by three phenyl rings on one side of the rhenium atom. The coordination geometry of the two compounds differ only by the interchange of the mutually *trans* chloro and carbonyl ligands. In (I) the carbonyl ligand is within the cavity and in (II) the chloro ligand is within the cavity.

Introduction

The reactions between $Mn(CO)_5X$ (X = Cl, Br, I) and the triphosphine $Ph_2P(CH_2)_2P(Ph)(CH_2)_2PPh_2$ (P_2P') have been investigated by two groups of workers. King and co-workers[4] synthesized $Mn(CO)_2(\eta^3\text{-}P_2P')Br$, while Butler and Coville[5,6] have prepared $Mn(CO)_3(\eta^2\text{-}P_2P')X$ and $Mn(CO)_2(\eta^3\text{-}P_2P')X$. The only structural information previously available for the dicarbonyl complexes is from the IR spectra which show the carbonyl groups to be *cis*.

In this paper, $Mn(CO)_2(\eta^3\text{-}P_2P')X$ and the previously unreported rhenium analogues $Re(CO)_2(\eta^3\text{-}P_2P')X$ (X = Cl, Br) compounds have been fully characterized by IR and multinuclear (^{31}P, ^{13}C) magnetic resonance spectroscopies. The electrochemical behavior of these complexes has been investigated on both the voltammetric and coulometric time scales and reveal the existence of relatively stable $[M(CO)_2(\eta^3\text{-}P_2P')X]^+$ complexes. The numerous isomerically related products of electrochemical and chemical redox reactions associated with the $[M(CO)_2(\eta^3\text{-}P_2P')X]^{+/0}$ system have been isolated and identified by a range of techniques, including multinuclear magnetic resonance and IR spectroscopies and electrospray mass spectrometry. X-ray crystallography has been used to characterize two novel diasteroisomers of *cis,mer*-$Re(CO)_2(\eta^3\text{-}P_2P')Cl$.

In all of the compounds described in this paper, the ligand P_2P' is bound to the metal as a tridentate ligand so the prefix η^3 will be omitted in all subsequent representations of the formulas.

Experimental Section

Materials and Preparations. All solvents were Analytical Reagent grade. Manganese and rhenium carbonyls and P_2P' (Strem) were used as supplied. The pentacarbonyl halides were prepared by interaction of the carbonyls with halogen.[7] $Mn(CO)_5X$ and 1 mol equiv of P_2P' were heated in refluxing xylene for 1 h. Upon cooling the solution, yellow needles (Cl) or orange needles (Br) separated out. The liquid was decanted off, and the needles were recrystallized from dichloromethane/hexane to give yellow needles of $Mn(CO)_2(P_2P')X$. $Re(CO)_5X$ and 1 mol equiv of P_2P' were heated in refluxing mesitylene for several

⊗ Abstract published in *Advance ACS Abstracts*, February 1, 1997.

(1) La Trobe University.
(2) Present address: Department of Chemistry, Monash University, Clayton, Victoria 3168, Australia.
(3) University of Melbourne.
(4) King, R. B.; Kapoor, P. N.; Kapoor, R. N. *Inorg. Chem.* **1971**, *10*, 1841.
(5) Butler, I. S.; Coville, N. J.; Spendjian, H. K. *J. Organomet. Chem.* **1972**, *43*, 185.
(6) Coville, N. J.; Butler, I. S. *J. Organomet. Chem.* **1973**, *57*, 355.
(7) Colton, R.; McCormick, M. J. *Aust. J. Chem.* **1976**, *29*, 1657.

S0020-1669(96)01295-5 CCC: $14.00

hours. Upon cooling the solution, a small amount of white solid precipitated and was filtered off and washed with hexane. Subsequently this solid was dissolved in dichloromethane and separated into five components by chromatography on silica as described in the text. Hexane was added to the filtered solution of mesitylene to precipitate a solid which was recrystallized from dichloromethane/hexane to yield crystals of $Re(CO)_2(P_2P')X$.

Electrochemical Methods. Conventional voltammetric measurements were typically obtained with 1.0 mM solutions of compound in dichloromethane (0.1 M Bu_4NPF_6) or acetone (0.1 M Bu_4NPF_6), using a Cypress Systems (Lawrence, KS) Model CYSY-1 computer controlled electrochemical system or a BAS 100A electrochemical analyzer (Bioanalytical Systems, West Lafayette, IN). The working electrode was a glassy carbon disk (0.5 mm radius), the auxiliary electrode was a platinum wire, and the reference electrode was Ag/AgCl (saturated LiCl in dichloromethane (0.1 M Bu_4NPF_6)) separated from the test solution by a salt bridge. The reversible voltammetry of an approximately 1.0 mM ferrocene (Fc) solution in the same solvents was used as a reference redox couple, and all potentials are quoted relative to Fc^+/Fc. Steady-state voltammograms were recorded using a 12.5 μm radius platinum microdisk electrode. Solutions were purged with solvent-saturated nitrogen before voltammetric measurements and then maintained under an atmosphere of nitrogen during measurements.

Bulk electrolysis experiments were undertaken with either a PAR Model 273 potentiostat or the BAS 100 A electrochemical analyzer using a large platinum basket working electrode and a platinum gauze auxiliary electrode separated from the test solution by a salt bridge and the same reference electrode as used in the voltammetric studies.

Spectroscopic Methods. NMR spectra were recorded on a Bruker AM 300 spectrometer, ^{31}P at 121.496 MHz in dichloromethane or acetone and ^{13}C at 75.469 MHz in $CDCl_3$ solution. The high-frequency positive convention is used for chemical shifts with external 85% H_3PO_4 and internal TMS references, respectively. Infrared spectra were recorded on a Perkin-Elmer FT-IR 1720X or a Perkin-Elmer 1430 IR spectrometer.

Electrospray Mass Spectrometry. Electrospray mass spectra of cationic complexes were obtained with a VG Bio-Q triple quadrupole mass spectrometer using a water/methanol/acetic acid (50:50:1) mobile phase. Solutions of the compounds (2.0 mM in dichloromethane) were mixed, if necessary, with oxidant or sodium acetate as described in the text. The mixed solution was then diluted 1:10 with methanol and immediately injected directly into the spectrometer via a Rheodyne injector fitted with a 10 μL loop. A Pheonix 20 micro LC syringe pump delivered the solution to the vaporization nozzle of the electrospray source at a flow rate of 5 μL min^{-1}. Nitrogen was used as the drying gas and for nebulization with flow rates of approximately 3 L min^{-1} and 100 mL min^{-1}, respectively. The voltage on the first skimmer (B1) was usually 40 V, but higher voltages were used to induce collisionally activated fragmentations as described in the text. Peaks are identified by the most abundant mass in the isotopic mass distribution. In all cases the agreement between experimental and theoretical isotopic mass patterns was good.

Crystal Structure Determinations for *cis,mer*-$Re(CO)_2(P_2P')Cl$(I)·CH_2Cl_2 and *cis,mer*-$Re(CO)_2(P_2P')Cl$(II). Crystallographic Data. Crystals of the two compounds identified as *cis,mer*-$Re(CO)_2(P_2P')Cl$ were obtained by slow evaporation of dichloromethane/hexane solutions of the complexes at room temperature. Intensity data were collected on an Enraf-Nonius CAD-4 Mach S diffractometer at 20 °C. Crystal data for both structures are given in Table 1.

Structure Determination and Refinement. Analytical absorption corrections were applied to the intensities before structure solution. The positions of the rhenium atoms were derived from vector maps, and the sites of the remaining non-hydrogen atoms were determined from successive difference maps using SHELX-76.[8] The structures were refined against F^2 with SHELX-93.[9] Hydrogen atoms were included at idealized positions using C−H bond lengths of 0.97 and 0.93 Å for the methylene and phenyl hydrogens, respectively. The thermal parameters of a Cl atom (Cl9) of one dichloromethane molecule in the structure of *cis,mer*-(I) indicated a strong libration. To approximate this effect, the coordinates of this atom were split into eight components and each given an occupancy factor of 0.125 (see Table 7). To decrease computational time only the 12 464 terms for which $I \geq 2\sigma I$ were used in the refinement of the structure of *cis,mer*-(I). Extinction corrections were not applied to the data, but one term (−1 0 2) was omitted from the final refinements of *cis,mer*-(II).

Table 1. Crystal Structure Data for Isomers of *cis,mer*-$Re(CO)_2(P_2P')Cl$

	cis,mer-(I)·CH_2Cl_2	*cis,mer*-(II)
formula	$C_{37}H_{35}Cl_3O_2P_3Re$	$C_{36}H_{33}ClO_2P_3Re$
M_r	897.1	812.2
color	colorless	colorless
cryst syst	monoclinic	monoclinic
space group	$P2_1/n$	$P2_1/c$
a, Å	18.749 (3)	13.898 (4)
b, Å	32.307 (6)	15.845 (1)
c, Å	18.978 (3)	15.443 (5)
β, deg	107.76 (2)	105.14 (1)
vol, Å^3	10 948 (7)	3283 (1)
Z	12	4
ρ(calc), g/cm^3	1.633	1.643
cryst dimens (distance in mm from centroid)	(−1 −2 1) 0.173 (1 2 −1) 0.226 (−1 −1 −2) 0.165 (121) 0.123 (−1 2 1) 0.140 (1 −2 −1) 0.140	(110) 0.12 (−1 −1 0) 0.12 (−1 1 0) 0.12 (1 −1 0) 0.12 (100) 0.107 (−1 0 0) 0.107 (001) 0.313 (0 0 −1) 0.313
temp, K	293	293
radiation, Å (graphite monochrometer)	Mo Kα (λ = 0.710 69)	Mo Kα (λ = 0.710 69)
F(000)	5328	1608
μ, cm^{-1}	37.1	40.1
transmn factors	max 0.4654, min 0.3434	max 0.5103, min 0.3700
2θ limits	$2.2 < 2\theta < 50.0$	$2.0 < 2\theta < 50.0$
no. of reflns collecd	18 769	6000
no. of unique reflns	16 453	5003
R_{amal}	0.0326	0.0303
no. of unique reflcns used ($I > 2\sigma(I)$)	12 464	4664
refinement	full matrix	full matrix
R_1[a]	0.0398	0.0187
R_w[b]	0.0863	0.0475
GOF[c]	1.008	1.059

[a] $R_{amal} = \sigma|F_o^2 - F_o^2(\text{mean})|/\sigma F_o^2$. $R_1 = \sum(|F_o| - |F_c|)/\sum|F_o|$. [b] $R_w = [\sum(F_o^2 - F_c^2)^2]/\sum_w F_o^2]\}^{1/2}$, where $w = [\sigma^2 F_o^2 + (0.0331P)^2 + 50.86P]^{-1}$ for *cis,mer*-(I) and $[\sigma^2 F_o^2 + (0.0296P)^2 + 0.9028P]^{-1}$ for *cis,mer*-(II) with $P = (F_o^2 + 2F_c^2)/3$. [c] GOF = $\{[\sum w(F_o^2 - F_c^2)]^2/(n - m)\}^{1/2}$, where n is the number of reflections used in the refinement and m is the number of parameters refined.

Results and Discussion

The chemistry of the $Mn(CO)_5X/P_2P'$ system is somewhat different to that of $Re(CO)_5X$ with P_2P', so it is convenient to describe the chemistry of the two metals separately.

A. Reactions of $Mn(CO)_5X$ with P_2P'. Spectroscopic evidence (Table 2) outlined below shows that the reaction of both carbonyl halides with P_2P' gives only a single isomer of the product previously characterized as $Mn(CO)_2(P_2P')X$. The infrared spectrum of $Mn(CO)_2(P_2P')Br$ shows two carbonyl stretches of approximately equal intensities, whose positions agree with literature values.[4,5] This spectrum shows that the carbonyl groups are mutually *cis*. Its ^{31}P NMR spectrum consists of two peaks of relative intensities 1:2, both of which are shifted considerably to high frequency compared with the positions of the resonances for the free ligand,[10] which confirms that all three phosphorus atoms are coordinated to the metal

(8) Sheldrick, G. M. *SHELX-76, Program for Crystal Structure Determination*; Cambridge University: Cambridge, U.K., 1976.
(9) Sheldrick, G. M. *SHELX-93, Program for the Refinement of Crystal Structures*; University of Göttingen: Germany, 1993.

Table 2. IR and NMR Data for All $[Mn(CO)_2(P_2P')X]^{+/0}$ Compounds

compound	ν_{CO}, cm^{-1}	$\delta(^{31}P)$,[a] ppm P′	$\delta(^{31}P)$,[a] ppm P_2	$\delta(^{13}C)$,[b] ppm	temp(NMR), °C
cis,mer-$Mn(CO)_2(P_2P')Cl$	1936, 1866	119.0	87.0	226[c]	22
cis,mer-$[Mn(CO)_2(P_2P')Cl]^+$	2033, 1960[d]				
cis,fac-$Mn(CO)_2(P_2P')Cl$		125.7	49.7		−80
cis,fac-$[Mn(CO)_2(P_2P')Cl]^+$	2052, 1060[d]				
trans-$Mn(CO)_2(P_2P')Cl$	1893	134.4	69.4		22
trans-$[Mn(CO)_2(P_2P')Cl]^+$	1973				
cis,mer-$Mn(CO)_2(P_2P')Br$	1936, 1866	119.0	85.9	227.1, 225.3	22
cis,mer-$[Mn(CO)_2(P_2P')Br]^+$	2031, 1960[d]				
cis,fac-$Mn(CO)_2(P_2P')Br$		129.2	49.5		−80
cis,fac-$[Mn(CO)_2(P_2P')Br]^+$	2048, 1960[d]				
trans-$Mn(CO)_2(P_2P')Br$	1893	137.3	70.1		22
trans-$[Mn(CO)_2(P_2P')Br]^+$	1970				

[a] In CH_2Cl_2 solution. [b] In $CDCl_3$ solution. [c] May be two overlapping resonances. [d] Value only approximate due to overlap with peak due to *trans*$^+$.

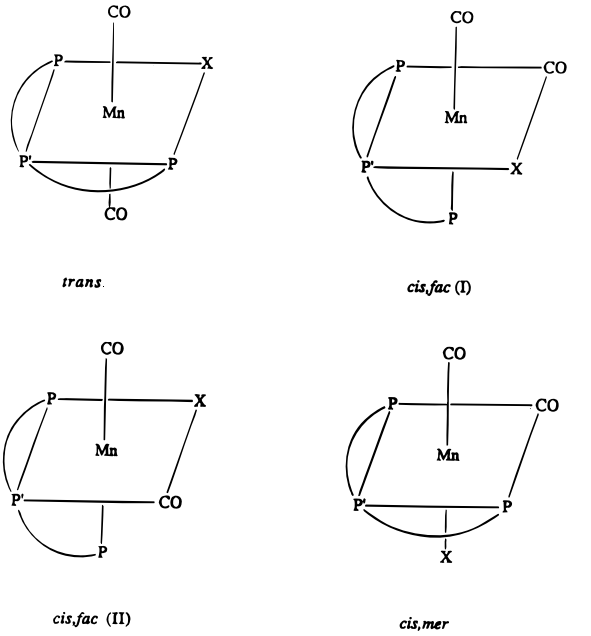

Figure 1. Four possible geometrical isomers of $Mn(CO)_2(P_2P')X$ (X = Cl, Br). The phenyl and methylene group have been omitted for clarity.

and also that the terminal phosphorus atoms remain chemically equivalent. Since it is known that P_2P' may coordinate to metals in both *fac* and *mer* configurations,[11] there are four possible isomers of $Mn(CO)_2(P_2P')X$, as shown in Figure 1, if only the geometry of the donor atoms about the metal is considered. The *trans* isomer is eliminated on the basis of the infrared spectrum and the *cis,fac*-(I) isomer is discarded on the basis of the ^{31}P NMR spectrum since it would have three non-equivalent phosphorus atoms. The *cis,fac*-(II) and *cis,mer* isomers may be distinguished by their ^{13}C NMR spectra (carbonyl region). The observed ^{13}C NMR spectrum of $Mn(CO)_2(P_2P')Br$ shows two carbonyl resonances which unequivocally determine the structure to be *cis,mer*. The spectroscopic data for $Mn(CO)_2(P_2P')Cl$ are very similar to those of *cis,mer*-$Mn(CO)_2(P_2P')Br$ except that the ^{13}C NMR spectrum shows only one resonance in the carbonyl region. However, the signal is rather broad and is probably two superimposed signals. Electrochemical data given below strongly indicate that both compounds are the same isomer, so it will be assumed that $Mn(CO)_2(P_2P')Cl$ is also *cis,mer*.

B. Electrochemical Studies. (i) Cyclic Voltammetry. All voltammetric data are summarized in Table 3; the potentials quoted are relative to the reversible $E^r_{1/2}$ value for the Fc^+/Fc couple. Unless stated otherwise, voltammograms were recorded using a 0.5 mm radius glassy carbon disk macroelectrode.

Figure 2a shows an oxidative cyclic voltammogram (scan rate, 200 mV s^{-1}) for a 1.0 mM solution of *cis,mer*-$Mn(CO)_2(P_2P')Cl$ in dichloromethane (0.1 M Bu_4NPF_6) at 20 °C. On the first scan an oxidative response (process 1) is observed and the corresponding reduction response (process 1′) is seen on the reverse scan. Second and subsequent scans are identical, and the response remains reversible at all scan rates (100−50 000 mV s^{-1}) and temperatures (−20 to +50 °C) examined. A steady-state voltammogram at a platinum disk microelectrode (radius, 12.5 μm) shows that the limiting current for process 1 is similar to that obtained for the oxidation of an equimolar solution of $Mn(CO)_3(dpe)Br$ (dpe = $Ph_2PCH_2CH_2PPh_2$), which is known[12] to be a one-electron oxidation. The redox process 1 may therefore be assigned as

$$\textit{cis,mer}\text{-}[Mn(CO)_2(P_2P')Cl]^+ + e^- \rightleftharpoons \textit{cis,mer}\text{-}Mn(CO)_2(P_2P')Cl \quad (1)$$

Figure 2b shows that at more positive potentials there are two further oxidation responses, both irreversible, a very small peak labeled process 2 and a larger response labeled process 3. These features will be discussed in more detail below.

In acetone (0.1 M Bu_4NPF_6) subtly different responses are observed in oxidative cyclic voltammograms of *cis,mer*-$Mn(CO)_2(P_2P')Cl$ at 20 °C. Figure 2c is a cyclic voltammogram (scan rate, 200 mV s^{-1}) over a limited potential range, and it shows only process 1 on the first oxidative scan, but on the reverse scan a small response (process 4′) is observed as well as process 1′. Second and subsequent scans under these conditions show an additional oxidative response (process 4). However, scans at −30 °C (scan rate, 200 mV s^{-1}) show only processes 1 and 1′, indicating that the formation of the species responsible for processes 4 and 4′ is a kinetically controlled step. This was confirmed by experiments at 20 °C using a scan rate of 5000 mV s^{-1}, and again processes 4 and 4′ were absent because the kinetically controlled reaction(s) was outrun by the electrochemical timescale.

Figure 2d shows an oxidative cyclic voltammogram (scan rate, 200 mV s^{-1}) at 20 °C for *cis,mer*-$Mn(CO)_2(P_2P')Cl$ in acetone (0.1 M Bu_4NPF_6) over a wider potential range. Processes 2 and 3 previously observed in dichloromethane are

(10) Colton, R.; Tedesco, V. *Inorg. Chim. Acta* **1992**, *202*, 95.
(11) Bond, A. M.; Colton, R.; Feldberg, S. W.; Mahon, P. J.; Whyte, T. *Organometallics* **1991**, *10*, 3320.
(12) Bond, A. M.; Colton, R.; McCormick, M. J. *Inorg. Chem.* **1977**, *16*, 155.

Table 3. Cyclic Voltammetric Data for Oxidation of *cis,mer*-$Mn(CO)_2(P_2P')X$ Compounds at a Glassy Carbon Disk Electrode

	cis,mer-$Mn(CO)_2(P_2P')Cl$					*cis,mer*-$Mn(CO)_2(P_2P')Br$				
process	scan rate, mV s^{-1}	E_p^{ox}, V vs Fc^+/Fc	E_p^{red}, V vs Fc^+/Fc	$E_{1/2}$,[a] V vs Fc^+/Fc	temp, °C	scan rate, mV s^{-1}	E_p^{ox}, V vs Fc^+/Fc	E_p^{red}, V vs Fc^+/Fc	$E_{1/2}$,[a] V vs Fc^+/Fc	temp, °C
				In Dichloromethane						
1	200	0.181	0.099	0.140	20	200	0.202	0.116	0.159	20
						200	0.196	0.108	0.152	−30
2	200	0.803			20	200	0.826			20
3	200	1.153			20	200	1.178			20
4		*b*				200	0.094	0.014	0.054	20
5	200	−0.391	−0.459	−0.425	20	200	−0.032	−0.108	−0.070	20
6	200	1.023			20	200	1.046			20
				In Acetone						
1	200	0.177	0.099	0.138	−30					
1	200	0.190	0.116	0.153	20	200	0.216	0.126	0.171	20
1	200	0.193	0.113	0.153	50	200	0.202	0.098	0.150	55
1	5000	0.216	0.106	0.161	20					
2	200	0.771			20	200	0.817			20
3	200	0.961			20	200	0.994			20
4	200	0.083	0.013	0.048	20	200	0.108	0.038	0.073	20
5	200	−0.375	−0.447	0.411	20	200	−0.368	−0.442	−0.405	20
6	200	1.073			20	200	1.054			20

[a] Calculated from the value of $(E_p^{ox} + E_p^{red})/2$, where E_p^{ox} and E_p^{red} are the oxidation and reduction peak potentials, respectively, associated with the designated processes under the stated conditions. [b] Process 4 cannot be observed in CH_2Cl_2 at 20 °C.

again observed, but process 2 is more pronounced in acetone. The relationship between processes 2 and 4 will be discussed later. Process 3, which is close to the solvent limit, remains irreversible at all temperatures and scan rates examined. It seems likely that process 3 is a further oxidation of *cis,mer*-$[Mn(CO)_2(P_2P')Cl]^+$ to a highly unstable 16-electron Mn(III) complex, thus explaining its irreversibility, and process 3 will not be considered further.

An oxidative cyclic voltammogram (scan rate, 200 mV s^{-1}) of *cis,mer*-$Mn(CO)_2(P_2P')Cl$ in acetone (0.1 M Bu_4NPF_6) at 55 °C does not exhibit process 4′, but there is a small new reductive response at −0.459 V vs Fc^+/Fc (process 5′) and the second and subsequent scans show the corresponding oxidation response at −0.391 V (process 5). Redox process 5 is a weak feature in the cyclic voltammograms of *cis,mer*-$Mn(CO)_2(P_2P')Cl$ but is more pronounced for *cis,mer*-$Mn(CO)_2(P_2P')Br$, and it will be discussed in more detail for that compound.

An oxidative cyclic voltammogram (scan rate, 200 mV s^{-1}) at 20 °C for *cis,mer*-$Mn(CO)_2(P_2P')Br$ in dichloromethane (0.1 M Bu_4NPF_6) as given in Figure 3a, shows processes 1 and 1′ as for *cis,mer*-$Mn(CO)_2(P_2P')Cl$, but process 4′ is also prominent, whereas this process was not observed for the chloro complex in this solvent. Process 2 (not shown) is also observed at more positive potentials. Process 4′ (and processes 4 and 2) can be removed by cooling the solution to −30 °C.

In acetone (0.1 M Bu_4NPF_6) under similar conditions, process 4′ is quite prominent on the first scan, as shown in Figure 3b, and the corresponding oxidative component (process 4) is seen on the second scan. On heating the acetone solution of *cis,mer*-$Mn(CO)_2(P_2P')Br$, cyclic voltammograms show that processes 1′ and 4′ shift closer together and at 40 °C appear as a single broad response, and the reduction response 5′ becomes apparent. At 55 °C the cyclic voltammogram of *cis,mer*-$Mn(CO)_2(P_2P')Br$ in acetone (Figure 3c) shows a much sharper response for processes 1 and 1′ (and 4, 4′) and processes 5′ and 5 are well-defined.

The compounds giving rise to processes 4 and 5 cannot be assigned on the basis of the cyclic voltammograms alone, but they are identified as other isomers of $Mn(CO)_2(P_2P')X$ on the basis of additional information obtained from the experiments described below.

(ii) Bulk Electrolysis. Exhaustive bulk oxidative electrolysis of a dichloromethane (0.4 M Bu_4NPF_6) solution of *cis,mer*-$Mn(CO)_2(P_2P')Cl$ was carried out at a platinum gauze working electrode at a potential of 0.270 V vs Fc^+/Fc (slightly more positive than process 1). The appearance of the solution changed from yellow to orange. A reductive cyclic voltammogram of the oxidized solution shows that process ($E_{1/2}$ = 0.142 V) is now absent, but a reversible couple is observed at −0.425 V vs Fc^+/Fc. This is the same potential as the small response labeled process 5 seen in the cyclic voltammograms for *cis,mer*-$Mn(CO)_2(P_2P')Cl$ in acetone (0.1 M Bu_4NPF_6) at 50 °C. Scanning to more positive potentials shows a new irreversible response at 1.023 V vs Fc^+/Fc (process 6), while processes 2 and 3 seen for *cis,mer*-$Mn(CO)_2(P_2P')Cl$ are absent. The voltammogram remains unchanged on the second and subsequent scans. The sign of the current in a steady-state voltammogram at a platinum microelectrode after the electrolysis shows that the species in solution giving rise to process 5 is in the oxidized form. Comparison of the limiting current with that for an equimolar solution of $Mn(CO)_3(dpm)Br$ shows that process 5 is a one-electron process. The IR spectrum of the oxidized solution exhibits a single peak in the carbonyl region at 1973 cm^{-1}.

Exhaustive bulk reductive electrolysis was then performed on the originally oxidized solution, and the color of the solution changed from orange to pink. A subsequent cyclic voltammogram shows the same redox couple for process 5, but a steady-state voltammogram at a platinum microelectrode shows that the species in solution is now in the reduced form. The IR spectrum of the reduced solution shows a single carbonyl absorption at 1893 cm^{-1}, and the ^{31}P NMR spectrum of the solution shows two signals (1:2). The IR data strongly indicates a *trans* configuration for the carbonyl groups, and the NMR spectrum is consistent with this formulation. Thus, process 5 is assigned to the redox couple

$$\textit{trans}\text{-}[Mn(CO)_2(P_2P')Cl]^+ + e^- \rightleftharpoons \textit{trans}\text{-}Mn(CO)_2(P_2P')Cl \quad (2)$$

Many previous studies[11−14] of group 6 and group 7 18-electron *cis*- or *fac*-carbonyl species have shown that upon

(13) Bond, A. M.; Colton, R.; Jackowski, J. J. *Inorg. Chem.* **1975**, *14*, 274.

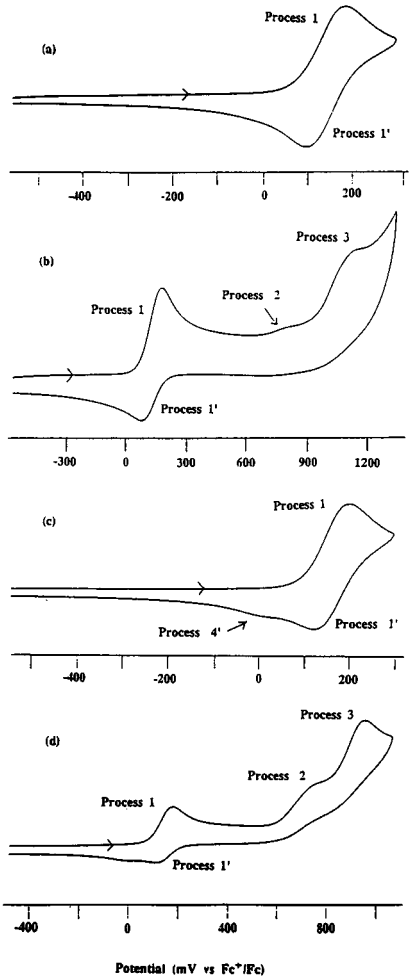

Figure 2. Oxidative cyclic voltammograms (scan rate, 200 mV s^{-1}) for 1 mM *cis,mer*-$Mn(CO)_2(P_2P')Cl$ solutions at a glassy carbon electrode (radius 0.5 mm) at 20 °C (a) in dichloromethane (0.1 M Bu_4NPF_6) over a restricted potential range, (b) under similar conditions, over an extended potential range, (c) in acetone (0.1 M Bu_4NPF_6) over a restricted potential range, and (d) similar conditions, over an extended potential range.

oxidation the resulting 17-electron species isomerize to the *trans*- or *mer*-carbonyl configuration, often on the voltammetric time scale. Thus, it is reasonable to observe a similar isomerization in the present case. In the present case the rate of isomerization is too slow to be observed on the voltammetric time scale at room temperature, but sufficiently fast for the isomerization to be complete on the electrolysis time scale. The overall reaction scheme may be represented by the following version of the square scheme

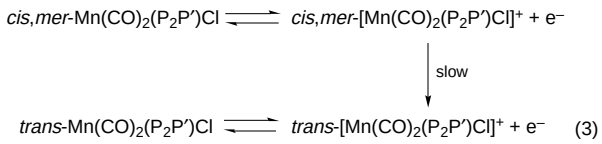

(3)

Isomerization of *trans*-$Mn(CO)_2(P_2P')Cl$ to *cis,mer*-$Mn(CO)_2(P_2P')Cl$ was not observed. Process 6 is due probably to further oxidation of *trans*-$[Mn(CO)_2(P_2P')Cl]^+$ to an unstable 16-electron Mn(III) species and will not be considered further. Exactly analogous observations were made for the bulk oxidation of *cis,mer*-$Mn(CO)_2(P_2P')Br$, and all data are given in Table 3.

(14) Bond, A. M.; Carr, S. W.; Colton, R. *Inorg. Chem.* **1984**, *23*, 2343.

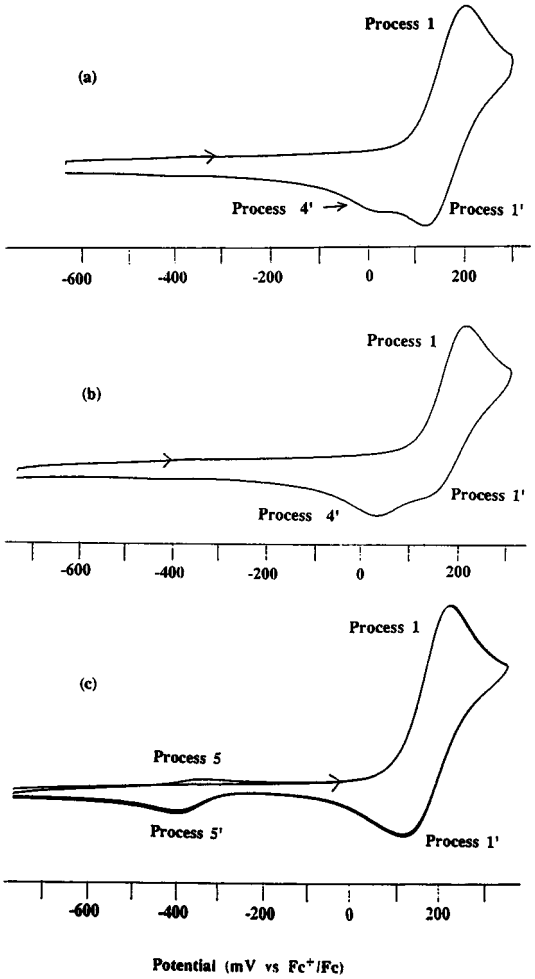

Figure 3. Oxidative cyclic voltammogram (scan rate, 200 mV s^{-1}) for 1 mM *cis,mer*-$Mn(CO)_2(P_2P')Br$ solutions at a glassy carbon electrode (radius 0.5 mm) (a) in dichloromethane (0.1 M Bu_4NPF_6) at 20 °C, (b) in acetone (0.1 M Bu_4NPF_6) at 20 °C, and (c) in acetone (0.1 M Bu_4NPF_6) at 55 °C.

C. Chemical Oxidation at Room Temperature. The chemical oxidants $NOBF_4$ and $(BrC_6H_4)_3NSbCl_6$ ("magic blue") were used to oxidize solutions of *cis,mer*-$Mn(CO)_2(P_2P')X$.

(i) Monitoring by IR Spectroscopy and Electrochemistry. Immediately after addition of $NOBF_4$ to a dichloromethane solution of *cis,mer*-$Mn(CO)_2(P_2P')Br$ the IR spectrum shows a weak peak at 2052 cm^{-1} and three strong absorptions at 2033, 1973 (assigned to *trans*-$[Mn(CO)_2(P_2P')Br]^+$), and 1960 cm^{-1} (shoulder). A reductive cyclic voltammogram of the solution, while all four IR peaks are present, shows the three reversible processes corresponding to processes 1, 4, and 5. However, after addition of the reductant cobaltocene to the oxidized solution, a voltammogram displays only processes 1 and 5, and the IR spectrum after reduction shows a stretch at 1893 cm^{-1} (assigned to *trans*-$Mn(CO)_2(P_2P')Br$) and also stretches at 1936 and 1866 cm^{-1} due to the starting material *cis,mer*-$Mn(CO)_2(P_2P')Br$.

When the IR spectrum of the solution containing *cis,mer*-$Mn(CO)_2(P_2P')Br$ and $NOBF_4$ is monitored over several minutes, the intensities of the peaks at 2052, 2033, and 1960 cm^{-1} decrease, while that of the stretch at 1973 cm^{-1} increases until this is the only peak in the spectrum. Reduction of this solution with cobaltocene gives an IR spectrum which contains only the stretch at 1893 cm^{-1} assigned to *trans*-$Mn(CO)_2(P_2P')Br$, as found for the bulk electrolysis experiments. Experiments in acetone give similar results as do those using magic blue as the oxidant, although in this case an irreversible reduction is

Table 4. Electrospray Mass Spectrometric Data at Low Ion Source Energies

compound	additive	ions (*m*/*z*)
cis,mer-$Mn(CO)_2(P_2P')Cl$	$NOBF_4$	$[Mn(CO)_2(P_2P')Cl]^+$ (680); $[Mn(CO)_2(P_2P')]^+$ (645); $[Mn(P_2P')Cl]^+$ (624)
cis,mer-$Mn(CO)_2(P_2P')Br$	$NOBF_4$	$[Mn(CO)_2(P_2P')Br]^+$ (726); $[Mn(P_2P')Br]^+$ (670); $[Mn(CO)_2(P_2P')]^+$ (645)
cis,mer-$Re(CO)_2(P_2P')Cl(I)$	$NOBF_4$	$[Re(CO)_2(P_2P')Cl]^+$ (812);[a] $[Re(CO)(NO)(P_2P')Cl]^+$ (814)[b]
	magic blue	$[Re(CO)_2(P_2P')Cl]^+$ (812)
cis,mer-$Re(CO)_2(P_2P')Br(I)$	$NOBF_4$	$[Re(CO)_2(P_2P')Br]^+$ (856);[a] $[Re(CO)(NO)(P_2P')Br]^+$ (858)[b]
	magic blue	$[Re(CO)_2(P_2P')Br]^+$ (856)
		$[Re(CO)_2(P_2P')Br_2]^+$ (937)
cis,mer-$Re(CO)_2(P_2P')Cl(I)$	Br_2	$[Re(CO)_2(P_2P')ClBr]^+$ (891)
cis,mer-$Re(CO)_2(P_2P')Br(I)$	Br_2	$[Re(CO)_2(P_2P')Br_2]^+$ (937)
cis,mer-$\{Re(CO)_2(P_2P')Cl\}_2$	magic blue	$[\{Re(CO)_2(P_2P')Cl\}_2]^+$ (1624)
	NaOAc	$[Na + \{Re(CO)_2(P_2P')Cl\}_2]^+$ (1647)
cis,mer-$Re(CO)_2(P_2P')Cl(II)$	$NOBF_4$	$[Re(CO)_2(P_2P')Cl]^+$ (812)
cis,mer-$Re(CO)_2(P_2P')Br(II)$	$NOBF_4$	$[Re(CO)_2(P_2P')Br]^+$ (856)

[a] Immediately after addition of $NOBF_4$. [b] Some minutes later.

observed close to the $trans^{+/0}$ couple which is assigned to the reduction of Sb(V) to Sb(III) from the anion of magic blue. The chloro complex *cis,mer*-$Mn(CO)_2(P_2P')Cl$ behaves similarly. Thus, chemical oxidation of *cis,mer*-$Mn(CO)_2(P_2P')X$ also produces *trans*-$[Mn(CO)_2(P_2P')X]^+$, which may be reduced to *trans*-$Mn(CO)_2(P_2P')X$, as in the bulk electrolysis experiments.

These experiments show that on the shorter time scale at least three oxidation products of *cis,mer*-$Mn(CO)_2(P_2P')X$ are present in solution and upon reduction after a short time *cis,mer*-$Mn(CO)_2(P_2P')X$ and *trans*-$Mn(CO)_2(P_2P')X$ are identified. This indicates that one likely oxidation product is *cis,mer*-$[Mn(CO)_2(P_2P')X]^+$. Longer time scale experiments show the isomerization of *cis,mer*-$[Mn(CO)_2(P_2P')X]^+$ to *trans*-$[Mn(CO)_2(P_2P')X]^+$ proceeds to completion as expected from previous studies of 17-electron carbonyl systems.[11−14] However, there is another species in solution (corresponding to process 4) which remains to be identified. The IR absorptions of this so far unidentified oxidation product and *cis,mer*-$[Mn(CO)_2(P_2P')X]^+$ cannot yet be assigned between the absorptions at 2052, 2033, and 1960 cm^{-1}.

(ii) ^{31}P NMR Spectroscopy. The ^{31}P NMR spectrum of a solution of *cis,mer*-$Mn(CO)_2(P_2P')Cl$ to which a small amount of $NOBF_4$ has been added consists of several broad peaks. However, when cobaltocene is added, the peaks become sharp and are resolved into the resonances for *cis,mer*-$Mn(CO)_2(P_2P')Cl$ and two new signals of relative intensities 1:2 which are assigned to *trans*-$Mn(CO)_2(P_2P')Cl$, previously identified from bulk electrolysis and chemical oxidation experiments. A similar experiment with isolated *trans*-$Mn(CO)_2(P_2P')Cl$ confirmed that its NMR peaks broadened on addition of magic blue, and after subsequent addition of cobaltocene only the sharp peaks of *trans*-$Mn(CO)_2(P_2P')Cl$ were observed in the spectrum. This experiment showed that no *trans* to *cis* isomerization occurs in either the 17- or 18-electron compounds on this time scale. Broadening of the NMR peaks of both *cis,mer*-$Mn(CO)_2(P_2P')Cl$ and *trans*-$Mn(CO)_2(P_2P')Cl$ in the solution of *cis,mer*-$Mn(CO)_2(P_2P')Cl$ after addition of $NOBF_4$ suggests that electron self-exchange is occurring between the 17- and 18-electron species, which is fast on the NMR time scale. Previous studies[14] have shown that fast electron exchange occurs only between isostructural species, and therefore it is likely that the broadening of the peaks of *cis,mer*-$Mn(CO)_2(P_2P')Cl$ is due to exchange with some *cis,mer*-$[Mn(CO)_2(P_2P')Cl]^+$ present in solution, rather than with the *trans*-$[Mn(CO)_2(P_2P')Cl]^+$ which is known to be present also.

(iii) Electrospray Mass Spectrometry. The electrospray mass spectra of solutions of both *cis,mer*-$Mn(CO)_2(P_2P')Cl$ and *cis,mer*-$Mn(CO)_2(P_2P')Br$ to which had been added some $NOBF_4$ both showed the appropriate intact cation $[Mn(CO)_2(P_2P')X]^+$ as the base peak in the mass spectrum, together with weaker peaks due to species formed by loss of either the two carbonyl groups or a halogen atom. Increasing the ion source energy increased the relative intensities of these fragment peaks, indicating that they are formed by collisions within the ion source. Although these spectra confirm that $[Mn(CO)_2(P_2P')X]^+$ ions exist in the oxidized solutions, they can give no information of the isomers present. All ESMS data are given in Table 4, where peaks are identified by the most abundant mass in the isotopic mass pattern. In all cases excellent agreement was observed between experimental and theoretical isotopic mass distributions.

D. Chemical Oxidation at Low Temperature. A steady-state voltammogram at a platinum microelectrode of a solution of *cis,mer*-$Mn(CO)_2(P_2P')Cl$ in dichloromethane (0.1 M Bu_4NPF_6) after oxidation with $NOBF_4$ at −30 °C shows process 1 as the dominant feature, and only a small response is observed for process 4. Low-temperature IR facilities are not available to us, but the IR spectrum recorded quickly at room temperature shows two strong absorptions at 2033 and 1960 cm^{-1} of approximately equal intensities, but there is also a small peak at 2052 cm^{-1}. These data strongly suggest that the strong absorptions at 2033 and 1960 cm^{-1} are due to the oxidized component of process 1, that is *cis,mer*-$[Mn(CO)_2(P_2P')Cl]^+$, while the weak peak at 2052 cm^{-1} is associated with the less abundant oxidative component of process 4. Monitoring the IR spectrum of this solution over several minutes at 20 °C reveals a decrease in these three peaks and a concomitant growth of a stretch at 1973 cm^{-1} due to *trans*-$[Mn(CO)_2(P_2P')Cl]^+$. However, the peaks at 2033 and 1960 cm^{-1} remain the same intensity relative to each other, confirming they are associated with the same compound.

When a sample of the oxidized solution which had been kept at −30 °C is reduced with cobaltocene at −30 °C, the IR spectrum shows only the peaks at 1936 and 1866 cm^{-1} due to *cis,mer*-$Mn(CO)_2(P_2P')Cl$, showing that the kinetically controlled isomerization which produces *trans*-$[Mn(CO)_2(P_2P')Cl]^+$ is slowed significantly so that no *trans*-$Mn(CO)_2(P_2P')Cl$ (ν_{CO} = 1893 cm^{-1}) is produced upon reduction with cobaltocene.

A steady-state voltammogram at a platinum microelectrode obtained at −25 °C of a solution originally containing *cis,mer*-$Mn(CO)_2(P_2P')Cl$ in acetone (0.1 M Bu_4NPF_6) after addition of $NOBF_4$ at −60 °C is similar to that observed in dichloromethane except that process 4 is enhanced. The IR spectrum of this solution shows a broad peak at 2032 cm^{-1} with a shoulder at ∼2050 cm^{-1} and a peak at 1959 cm^{-1}. The peaks at 2032 and 1959 cm^{-1} have already been assigned to *cis,mer*-$[Mn(CO)_2(P_2P')Cl]^+$, and the peak at 2050 cm^{-1} is stronger than in dichloromethane, confirming that it is associated with the more abundant oxidized species associated with process 4.

Table 5. IR and NMR Data for All $[Re(CO)_2(P_2P')X]^{+/0}$ Compounds

compound	ν_{CO},[a] cm^{-1}		$\delta(^{31}P)$,[a] ppm P′	$\delta(^{31}P)$,[a] ppm P_2	$\delta(^{13}C)$,[b] ppm		coupling constants, Hz
cis,mer-$Re(CO)_2(P_2P')Cl$(I)	1941	1855	75.6	35.0	201.6d	196.5	$J_{C-P} = 56$
cis,mer-$Re(CO)_2(P_2P')Cl$(II)	1949	1860	56.7	27.0	202.5d	189.9	$J_{C-P} = 62$
cis,fac-$Re(CO)_2(P_2P')Cl$	1950	1886	66.9	10.7			
trans-$Re(CO)_2(P_2P')Cl$	1906		78.5	19.6			
trans-$[Re(CO)_2(P_2P')Cl]^+$	1968						
cis,mer-$\{Re(CO)_2(P_2P')Cl\}_2$	1941	1862	21.2	38.2d, 0.8d			$J_{P-P} = 180$
fac-$[Re(CO)_3(P_2P')]Cl$	2040	1962	65.7	27.6			
cis,mer-$Re(CO)_2(P_2P')Br$(I)	1941	1860	74.0	32.6	200.9d	195.8	$J_{C-P} = 49$
cis,mer-$Re(CO)_2(P_2P')Br$(II)	1950	1862	53.7	25.1	201.9d	189.4	$J_{C-P} = 54$
cis,fac-$Re(CO)_2(P_2P')Br$	1951	1888	67.8	8.6			
trans-$Re(CO)_2(P_2P')Br$	1906		78.2	18.5			
trans-$[Re(CO)_2(P_2P')Br]^+$	1967						
cis,mer-$\{Re(CO)_2(P_2P')Br\}_2$	1942	1862	21.2	38.0d, 0.2d			$J_{P-P} = 180$
fac-$[Re(CO)_3(P_2P')]Br$	2040	1962					

[a] In CH_2Cl_2 solution. [b] In $CDCl_3$ solution.

Reduction of this solution with cobaltocene was undertaken at −60 °C, and the resulting steady-state voltammogram shows that process 4 is still present, but now in the reduced form. The reduced solution was kept at low temperature, and the ^{31}P NMR spectrum was acquired at −80 °C. It shows resonances at δ 119.0 and 87.0 ppm due to *cis,mer*-$Mn(CO)_2(P_2P')Cl$ and two other signals of 1:2 relative intensities occur at δ 125.7 and 49.7 ppm. When the solution is allowed to warm to room temperature, the NMR spectrum of the solution then shows only the resonances due to *cis,mer*-$Mn(CO)_2(P_2P')Cl$. This result shows that the reduced form associated with process 4 is another isomer of $Mn(CO)_2(P_2P')Cl$ which is stable only at low temperature and rapidly converts to *cis,mer*-$Mn(CO)_2(P_2P')Cl$ near room temperature. Similar experiments with *cis,mer*-$Mn(CO)_2(P_2P')Br$ in acetone give analogous spectra, and all data are recorded in Tables 2 and 3. As noted earlier, *cis,fac*-(I) would give three resonances in its ^{31}P NMR spectrum, while the *cis,fac*-(II) isomer would give only two resonances (1:2 intensities). Unfortunately, both *cis,fac* isomers of $[Mn(CO)_2(P_2P')X]^+$ should have two carbonyl stretches in the IR spectrum, but only one is observed, and it is assumed that the second is obscured by the absorption due to *cis,mer*-$[Mn(CO)_2(P_2P')X]^+$ at 1960 cm^{-1}. Attempts to observe the IR spectrum of *cis,fac*-$Mn(CO)_2(P_2P')X$ were unsuccessful due the rapid isomerization to *cis,mer*-$Mn(CO)_2(P_2P')X$. Despite the difficulty with the IR spectrum, the balance of evidence suggests that process 4 can be assigned to the redox couple

$$\textit{cis,fac}\text{-}Mn(CO)_2(P_2P')X(II) \rightleftharpoons \textit{cis,fac}\text{-}[Mn(CO)_2(P_2P')X(II)]^+ + e^- \quad (4)$$

The corresponding rhenium complex, *cis,fac*-$Re(CO)_2(P_2P')X(II)$, which is more stable and has been fully characterized (see later), displays similar redox properties.

As shown in Figure 2, process 4 appears for the first time on the reverse scan in the voltammetry of *cis,mer*-$Mn(CO)_2(P_2P')X$, and therefore the *cis,fac*-(II) isomer is generated in the 17-electron configuration. However, the isomerization does not proceed to completion (since process 1′ is also present on reverse scans). In fact, at 55 °C in acetone this isomerization reaction in both directions is so fast that on the electrochemical time scale the observed response becomes an average of processes 1 and 4. Similar fast isomerizations have previously been observed for other P_2P' complexes.[11] The experiments described above prove that in the 18-electron configuration *cis,fac*-(II) rapidly isomerizes to *cis,mer*. The overall reactions may therefore be summarized in a square reaction scheme

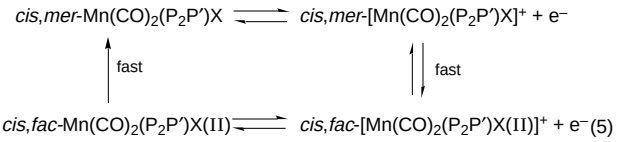

As described earlier in the voltammetry section, the use of fast scan rates or lowering the temperature leads to the disappearance of both processes 2 and 4 in the cyclic voltammograms of *cis,mer*-$Mn(CO)_2(P_2P')X$. This suggests that these processes are both associated with the same compounds, and process 2, which will not be considered further, is most likely further oxidation of *cis,fac*-$[Mn(CO)_2(P_2P')X]^+$ to an unstable 16-electron Mn(III) species

$$\textit{cis,fac}\text{-}[Mn(CO)_2(P_2P')X(II)]^+ \rightarrow \textit{cis,fac}\text{-}[Mn(CO)_2(P_2P')X(II)]^2 + e^- \quad (6)$$

E. Reactions of $Re(CO)_5X$ with P_2P'. It was found that $Re(CO)_5X$ compounds did not react with P_2P' at a reasonable rate in refluxing xylene, but reaction did occur in refluxing mesitylene solution. Upon cooling the solution to room temperature, a small amount of precipitate was formed but the bulk of the material remained in solution. The precipitate was filtered off, and its composition will be discussed later after the identity of the soluble material has been established and its oxidative chemistry described.

The IR spectrum of the mesitylene solution following reaction of $Re(CO)_5Cl$ and P_2P' shows two carbonyl stretches of equal intensities at 1941 and 1855 cm^{-1}. These positions are similar to those of *cis,mer*-$Mn(CO)_2(P_2P')Cl$ and indicate *cis*-carbonyl groups. The ^{31}P NMR spectrum shows two signals (1:2) both shifted to higher frequency than the resonances of the free ligand, confirming all the phosphorus atoms are coordinated to rhenium. Addition of hexane to the mesitylene solution caused the precipitation of a white compound which was recrystallized from dichloromethane/hexane. The ^{13}C NMR spectrum of this compound dissolved in deuterochloroform exhibits two resonances of equal intensities in the carbonyl region at δ 201.6 and 196.5 ppm, showing that the stereochemistry is *cis,mer*. The ^{13}C NMR signal at higher frequency appears as a doublet ($J_{C-P} = 56$ Hz) and is therefore assigned to the carbon atom of the carbonyl group *trans* to P′. The spectroscopic data indicate the stereochemistry is the same as that for the manganese complex, and this geometry has been confirmed in the solid state by a crystal structure determination. Spectroscopic data are similar for *cis,mer*-$Re(CO)_2(P_2P')Br$, and details are given in Table 5, but in the table the compounds are referred to as

cis,mer-$Re(CO)_2(P_2P')X(I)$ to distinguish them from another isomer which will be described later.

F. Electrochemical Studies. (i) Cyclic Voltammetry. The general features of the voltammetry of *cis,mer*-$Re(CO)_2(P_2P')X$ are similar to those of the manganese analogues, and only a generalized description will be given. All voltammetric data are given in Table 6, and the electrochemical processes are given the same numbers as the corresponding processes for the manganese complexes. Process 4 for *cis,mer*-$Re(CO)_2(P_2P')$-Cl is weak in dichloromethane but more pronounced in acetone and also more pronounced for the bromo complex, as was found for the manganese complexes. The behavior of process 4 with temperature also parallels the behavior previously described for solutions of *cis,mer*-$Mn(CO)_2(P_2P')X$.

(ii) Bulk Electrolysis. Exhaustive oxidative bulk electrolysis of a dichloromethane (0.4 M Bu_4NClO_4) solution of *cis,mer*-$Re(CO)_2(P_2P')Br(I)$ was undertaken at 20 °C at a platinum working electrode and a potential of 0.400 V vs Fc^+/Fc. Monitoring by steady-state voltammetry during the course of the electrolysis indicates that *cis,mer*-$[Re(CO)_2(P_2P')Br(I)]^+$ is not stable on the longer coulometric time scale since no reductive component was present for the redox couple 1, only the oxidative component due to not yet oxidized *cis,mer*-$Re(CO)_2(P_2P')Br$ being observed. The reductive component of process 4 was also present together with process 5. The limiting current associated with process 5 increased as the electrolysis proceeded, but gradually other responses at more negative potentials became dominant. Depending upon the experimental conditions (concentration of *cis,mer*-$Re(CO)_2(P_2P')Cl$, time of electrolysis) the charge passed after exhaustive electrolysis was between 1 and 2 electrons per molecule. Similar observations were made in acetone, with Bu_4NPF_6 as the supporting electrolyte and for the chloro complex *cis,mer*-(I).

A bulk electrolysis of *cis,mer*-$Re(CO)_2(P_2P')Br(I)$ in acetone (0.1 M Bu_4NClO_4) was undertaken at −40 °C in an attempt to prevent decomposition of the species associated with process 5. The responses at more negative potentials still appeared on the longer time scale (at least 1 h) at this temperature, but a greater proportion of the total current was associated with process 5 than at room temperature. The oxidative electrolysis was stopped prior to completion so that a subsequent reductive bulk electrolysis could be undertaken while a significant amount of the species responsible for process 5 was still present. Before reduction the IR spectrum of the solution shows an absorption at 1969 cm^{-1} as well as the bands at 1941 and 1860 cm^{-1} of unoxidized *cis,mer*-$Re(CO)_2(P_2P')Br(I)$. After exhaustive reductive bulk electrolysis at −0.150 V vs Fc^+/Fc at −40 °C a steady-state voltammogram shows process 5 is now in the reduced form. A similar voltammogram recorded after the solution had warmed to 20 °C shows that the relative currents for processes 1 and 5 had not changed. The ^{31}P NMR spectrum of the reduced solution shows a number of peaks. The solution was evaporated to dryness, the solid was redissolved in dichloromethane, and the solution was then passed through a column of silica gel. The ^{31}P NMR spectrum of the eluant shows resonances due to *cis,mer*-$Re(CO)_2(P_2P')Br(I)$ at δ 74.0 and 32.6 ppm and two other peaks (1:2) at δ 78.2 and 18.5 ppm. The IR spectrum now shows a strong absorption at 1906 cm^{-1}. All of this evidence confirms that the redox process 5 is due to

$$\textit{trans}\text{-}[Re(CO)_2(P_2P')Br]^+ + e^- \rightleftharpoons \textit{trans}\text{-}Re(CO)_2(P_2P')Br \quad (7)$$

analogous to the manganese system, but there are side reactions not observed with manganese.

The fact that more than one electron per molecule is consumed in the oxidative electrolysis is consistent with a disproportionation reaction of the 17e species. In group 6 carbonyl chemistry there are many examples of relatively stable chromium 17e species, but the corresponding Mo(I) and W(I) complexes disproportionate to M(0) and M(II).[15] This reaction is assisted by the stability of seven-coordinate, 18e, M(II) complexes. Although the chemistry of seven-coordinate Re(III) is not as well-explored as that of Mo(II) and W(II), a significant number of compounds are known[16] and a similar disproportionation reaction is not unexpected.

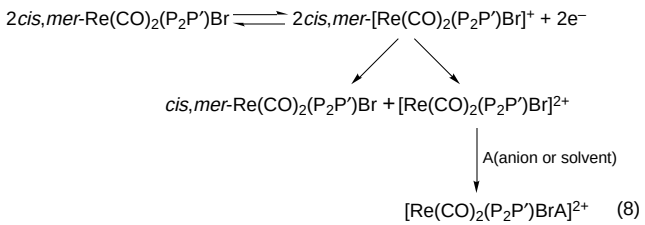

This disproportionation reaction of *cis,mer*-$[Re(CO)_2(P_2P')Br]^+$ would be in competition with the isomerization to *trans*-$[Re(CO)_2(P_2P')Br]^+$ and would lead to a mixture of products if their rates were comparable. The experiments described so far do not prove the existence of a disproportionation reaction, but the consumption of more than one electron and the dependence of electrolysis products on concentration do strongly support the suggestion. Positive proof for the formation of Re(III) species by chemical oxidation was obtained by ESMS.

G. Electrospray Mass Spectrometry. All ESMS data are given in Table 4. The ES mass spectrum (B1 = 40 V) of a solution of *cis,mer*-$Re(CO)_2(P_2P')Cl$ after addition of $NOBF_4$ shows a strong peak for the intact ion $[Re(CO)_2(P_2P')Cl]^+$ (*m*/*z* 812) provided the mass spectrum is acquired immediately after addition of the oxidant. However, if the solution is allowed to stand for a few minutes before injection into the spectrometer, the signal at *m*/*z* 812 is not detected but instead a peak at *m*/*z* 814 is observed, which is assigned to the intact ion $[Re(CO)(NO)(P_2P')Cl]^+$. This cation is formed by reaction of NO with the 17-electron dicarbonyl cation, and similar reactions have been observed previously.[17] When magic blue is used to oxidize *cis,mer*-$Re(CO)_2(P_2P')Cl$, only $[Re(CO)_2(P_2P')Cl]^+$ is observed. Collisionally activated fragmentation of $[Re(CO)(NO)(P_2P')Cl]^+$ can be observed by increasing the B1 voltage. At B1 = 70 V loss of carbonyl is observed, and at B1 = 90 V $[Re(NO)(P_2P')]^+$ (*m*/*z* 751) and $[Re(NO)(P_2P'O)]^+$ (*m*/*z* = 767) are observed. The phosphine oxide in the latter ion is formed within the ion source, and this reaction is commonly observed in the ES mass spectra of phosphine complexes.[18] When B1 = 110 V, the peaks at *m*/*z* 751 and 767 are dominant, but a peak for the intact ion $[Re(CO)(NO)(P_2P')Cl]^+$ is still present, indicating its considerable stability. Analogous ES mass spectra were observed when *cis,mer*-$Re(CO)_2(P_2P')Br$ was oxidized with $NOBF_4$ and magic blue, except that with the latter oxidant in addition to the major peak at *m*/*z* 856 due to $[Re(CO)_2(P_2P')Br]^+$, a small peak was observed at *m*/*z* 937 which is assigned to the seven-coordinate Re(III) cation $[Re(CO)_2(P_2P')Br_2]^+$. This

(15) (a) Bond, A. M.; Bowden, J. A.; Colton, R. *Inorg. Chem.* **1974**, *13*, 602. (b) Bond, A. M.; Colton, R.; Kevekordes, J. E.; Panagiotidou, P. *Inorg. Chem.* **1987**, *26*, 1430.
(16) *Comprehensive Organometallic Chemistry*; Wilkinson, G., Stone, F. G. A., Abel, E. W., Eds.; Pergamon Press: Oxford, U.K., 1982.
(17) Connelly, N. G. *J. Chem. Soc., Dalton Trans.* **1973**, 2183.
(18) (a) Colton, R.; Harvey, J.; Traeger, J. C. *Org. Mass. Spectrom.* **1992**, *27*, 95. (b) Colton, R.; Dakternieks, D. *Inorg. Chim. Acta* **1993**, *208*, 173.

Table 6. Cyclic Voltammetric Data for Oxidation of *cis,mer*-$Re(CO)_2(P_2P')X$ Compounds at a Glassy Carbon Disk Electrode[a] (Scan Rate, 200 mV s^{-1})

	cis,mer-$Re(CO)_2(P_2P')Cl$			*cis,mer*-$Re(CO)_2(P_2P')Br$		
process[b]	E_p^{ox}, V vs Fc^+/Fc	E_p^{red}, V vs Fc^+/Fc	$E_{1/2}$, V vs Fc^+/Fc	E_p^{ox}, V vs Fc^+/Fc	E_p^{red}, V vs Fc^+/Fc	$E_{1/2}$, V vs Fc^+/Fc
			In Dichloromethane			
1	0.551	0.461	0.506	0.556	0.472	0.514
2	1.018					
3	1.050			1.002		
4	0.378	0.300	0.339	0.382	0.302	0.342
5	−0.039	−0.113	0.076	0.006	−0.108	−0.051
cis,mer-(II)	0.440	0.352	0.396	0.445	0.359	0.402
compound **A**	0.522	0.442	0.482	0.529	0.447	0.488
	0.646	0.568	0.607	0.657	0.577	0.615
			In Acetone			
1	0.567	0.489	0.528	0.570	0.480	0.525
4	0.391	0.333	0.362	0.396	0.340	0.368
5	−0.046	−0.116	−0.081	−0.044	−0.114	−0.079
cis,mer-(II)	0.448	0.372	0.410	0.453	0.379	0.416

[a] Symbols have the same meaning as in Table 3. [b] Perocesses 1−5 refer to *cis,mer*-(I) and have the same assignments as for the manganese compounds.

observation led to an investigation by ESMS of the oxidation of *cis,mer*-$Re(CO)_2(P_2P')X$ with bromine.

The ES mass spectrum (B1 = 40 V) of a solution of *cis,mer*-$Re(CO)_2(P_2P')Cl$ after addition of a little bromine does not give a peak for $[Re(CO)_2(P_2P')Cl]^+$ (*m/z* 812), but instead a peak is observed at *m/z* 891 which is due to $[Re(CO)_2(P_2P')ClBr]^+$. At higher collision energies one carbonyl group is lost. Oxidation of *cis,mer*-$Re(CO)_2(P_2P')Br$ with bromine gave an analogous spectrum with a strong peak at *m/z* 937 due to $[Re(CO)_2(P_2P')Br_2]^+$. This oxidation of *cis,mer*-$Re(CO)_2(P_2P')X$ with bromine closely resembles the formation of $[M(CO)_2(P{-}P)_2X]^+$ cations (M = Mo, W; P−P = diphosphine) by halogen oxidation of $M(CO)_2(P{-}P)_2$.[19]

H. Other Derivatives of $Re(CO)_5X$ with P_2P'. The precipitate obtained from the reaction between $Re(CO)_5Cl$ and P_2P' was dissolved in dichloromethane. The IR spectrum in the carbonyl region consists of several overlapping absorptions, and the ^{31}P NMR spectrum of the solution displays many resonances. The relative intensities of these signals vary between preparations and also depend upon the reaction time, which indicates that the solution contains a mixture of products. However, for long reflux times (>24 h) the ^{31}P NMR spectrum shows only the signals due to *cis,mer*-$Re(CO)_2(P_2P')Cl(I)$.

The components of the mixture were separated by chromatography using a column of silica. Upon elution with dichloromethane and acetone a total of five compounds were isolated from the original small amount of precipitate and identified. The second compound to be eluted was *cis,mer*-$Re(CO)_2(P_2P')Cl(I)$, already identified as the major product of the reaction. The other four compounds (**A**−**D**) are identified as follows, and similar products were obtained from the reactions between $Re(CO)_5Br$ and P_2P'.

(i) Compound A. The first compound to be eluted with dichloromethane was obtained in only very small amounts. Its IR spectrum shows two bands at 1941 and 1862 cm^{-1}, indicating a *cis*-dicarbonyl structure. The ^{31}P NMR spectrum consists of three resonances of equal intensities, but two of the signals are split into doublets with a coupling constant of 180 Hz, which is a typical value for *trans* coupling between inequivalent phosphorus atoms on Re(I).[20] This spectrum shows that there must be two P_2P' ligands in the molecule, and the spectroscopic data are consistent with the dimeric *cis,mer* stereochemistry shown in Figure 4. An oxidative cyclic voltammogram of a dichloromethane (0.1 M Bu_4NPF_6) solution of compound **A** shows two reversible couples (Table 6) separated by 125 mV, which is typical behavior for dinuclear complexes,[21,22] and there are additional irreversible processes at higher positive potentials. A steady-state voltammogram for the two reversible processes shows that the limiting currents are equal and similar to the value obtained for the two reversible one-electron oxidations for an equimolar solution of *mer,mer*-$\{Cr(CO)_3(\eta^2\text{-dpe})\}_2(\mu\text{-dpe})$.[22] Thus these processes correspond to the consecutive oxidations of the two rhenium atoms (eqs 7 and 8), and the separation between the oxidation potentials suggests electronic communication between the metal centers.

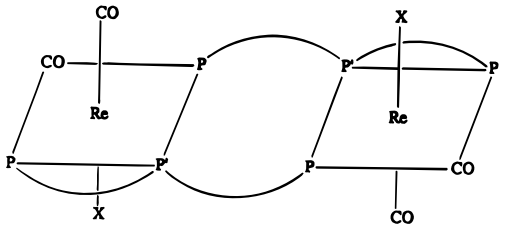

Figure 4. Proposed structure for *cis,mer*-$\{Re(CO)_2(P_2P')X\}_2$.

$$cis,mer\text{-}[\{Re(CO)_2(P_2P')Cl\}_2]^+ + e^- \rightleftharpoons cis,mer\text{-}\{Re(CO)_2(P_2P')Cl\}_2 \quad (9)$$

$$cis,mer\text{-}[\{Re(CO)_2(P_2P')Cl\}_2]^{2+} + e^- \rightleftharpoons cis,mer\text{-}[\{Re(CO)_2(P_2P')Cl\}_2]^+ \quad (10)$$

Unfortunately, bulk electrolysis experiments could not be carried out on compound **A** due to the small amount of material available.

(19) (a) Snow, M. R.; Wimmer, F. *Aust. J. Chem.* **1976**, *29*, 2349. (b) Ahmed, I.; Bond, A. M.; Colton, R.; Jurcevic, M.; Traeger, J. C.; Walter, J. N. *J. Organomet. Chem.* **1993**, *447*, 59.

(20) Carr, S. W.; Fontaine, X. L. R.; Shaw, B. L. *J. Chem. Soc., Dalton Trans.* **1987**, 3067.

(21) (a) Van Order, N.; Geiger, W. E.; Bitterwolf, T. E.; Rheingold, A. L. *J. Am. Chem. Soc.* **1987**, *109*, 5680. (b) Sullivan, B. T.; Meyer, T. J. *Inorg. Chem.* **1980**, *19*, 752. (c) Kober, E. M.; Goldsby, K. A.; Narayana, D. N. S.; Meyer, T. J. *J. Am. Chem. Soc.* **1983**, *105*, 4303.

(22) Bond, A. M.; Colton, R.; Cooper, J. B.; McGregor, K.; Walter, J. N.; Way, D. M. *Organometallics* **1995**, *14*, 49.

Conclusive proof of the dimeric nature of compound **A** was obtained from ESMS studies. The ES mass spectrum of a solution of compound **A** after addition of a small amount of magic blue gave a weak peak at *m*/*z* 1624, which corresponds to the intact ion $[\{Re(CO)_2(P_2P')Cl\}_2]^+$. This peak is probably weak because magic blue would oxidize most of the compound beyond $[\{Re(CO)_2(P_2P')Cl\}_2]^+$. Much more positive evidence for the dimeric structure was obtained by addition of sodium acetate to a solution of compound **A**, and the ES mass spectrum gave a strong peak for the sodium adduct $[Na + \{Re(CO)_2(P_2P')Cl\}_2]^+$ at *m*/*z* 1647. On the basis of the above evidence, compound **A** can be identified as *cis*,*mer*-$\{Re(CO)_2(P_2P')Cl\}_2$ with the structure shown in Figure 4.

The second complex eluted from the silica column with dichloromethane was identified by its IR and ^{31}P NMR spectra as *cis*,*mer*-$Re(CO)_2(P_2P')Cl(I)$.

(ii) Compound B. Further elution with dichloromethane gave a third species (compound **B**) which also displays two carbonyl absorptions in its IR spectrum. The ^{31}P NMR spectrum shows two resonances (1:2), and the ^{13}C NMR spectrum shows two carbonyl resonances with the higher frequency signal appearing as a doublet with a coupling constant similar to that observed for *cis*,*mer*-$Re(CO)_2(P_2P')Cl(I)$. All of the spectra are similar to those of *cis*,*mer*-$Re(CO)_2(P_2P')Cl(I)$, although the actual values are quite distinguishable from those of the major product (Table 5). The ES mass spectrum of a solution of compound **B** after addition of $NOBF_4$ gave a strong peak at *m*/*z* 812 which corresponds to the intact monomeric ion $[Re(CO)_2(P_2P')Cl]^+$. Thus, the spectroscopic and mass spectral data suggest the compound is another form of *cis*,*mer*-$Re(CO)_2(P_2P')Cl$ but the difference between the two forms was not obvious. Accordingly, crystal structures were determined for these compounds, and both were indeed found to be *cis*,*mer*-$Re(CO)_2(P_2P')Cl$. The two isomers arise from differences associated with the phenyl rings of P_2P' and will be discussed in the next section. To distinguish the isomers, the major product will henceforth be referred to as *cis*,*mer*-$Re(CO)_2(P_2P')Cl(I)$ and the minor product as *cis*,*mer*-$Re(CO)_2(P_2P')Cl(II)$.

One difference between the *cis*,*mer* isomers is seen in the oxidative voltammetry. For a solution of *cis*,*mer*-$Re(CO)_2(P_2P')Cl(II)$ in dichloromethane (0.1 M Bu_4NPF_6) a reversible redox couple (process 1) is observed together with a further irreversible oxidation (process 3) at more positive potential, but there is no indication of process 4′, in contrast to the behavior observed for *cis*,*mer*-$Re(CO)_2(P_2P')Cl(I)$. This difference is significant and will be discussed later.

(iii) Compound C. Compound **C** was removed from the column using acetone as the eluant after removal of compounds **A** and **B** and *cis*,*mer*-$Re(CO)_2(P_2P')Cl(I)$ with dichloromethane. Its IR and ^{31}P NMR spectra are identical to those observed after *cis*,*mer*-$Re(CO)_2(P_2P')Cl(I)$ is first chemically oxidized and then the solution reduced at low temperature, so compound **C** is identified as *cis*,*fac*-$Re(CO)_2(P_2P')Cl(II)$. Clearly this compound is kinetically more stable than its manganese analogue, which could only be observed at low temperature in the presence of *cis*,*mer*-$Mn(CO)_2(P_2P')Cl$.

The IR spectrum of *cis*,*fac*-$Re(CO)_2(P_2P')Cl(II)$ shows two carbonyl stretches at 1950 and 1880 cm^{-1}. After addition of a very small amount of magic blue (insufficient to oxidize all the compound in solution), the IR spectrum shows stretches at 1941 and 1855 cm^{-1} and the ^{31}P NMR spectrum shows resonances at δ 75.6 and 35.0 ppm. These spectroscopic data reveal that the species in solution is now *cis*,*mer*-$Re(CO)_2(P_2P')Cl(I)$. The first scan of a cyclic voltammogram of *cis*,*fac*-$Re(CO)_2(P_2P')Cl(II)$ in dichloromethane (0.1 M Bu_4NPF_6) shows the expected reversible process 4 but also another smaller reversible response identified as process 1. At more positive potentials the irreversible oxidation responses previously called processes 2 and 3 are also present. On the second scan the peak height of process 1 is now greater than that of process 4. After several hours a cyclic voltammogram shows only processes 1 and 3, both of which are associated with *cis*,*mer*-$Re(CO)_2(P_2P')Cl(I)$. Thus, addition of a small amount of oxidant or simply recording a cyclic voltammogram (which generates very small amounts of oxidized species) is sufficient to convert *cis*,*fac*-$Re(CO)_2(P_2P')Cl(II)$ to *cis*,*mer*-$Re(CO)_2(P_2P')Cl(I)$. This type of behavior has been observed before[23] and can be attributed to a catalytic process as follows. Oxidation of the *cis*,*fac*-(II) isomer with a small quantity of oxidant generates *cis*,*fac*$^+$ which rapidly isomerizes to *cis*,*mer*$^+$. The cross redox reaction

$$cis,fac\text{-}Re(CO)_2(P_2P')Cl + cis,mer\text{-}[Re(CO)_2(P_2P')Cl]^+ \rightleftharpoons cis,mer\text{-}Re(CO)_2(P_2P')Cl + cis,fac\text{-}[Re(CO)_2(P_2P')Cl]^+ \quad (11)$$

then occurs between *cis*,*mer*$^+$ and the remaining *cis*,*fac*, which generates *cis*,*mer* and more *cis*,*fac*$^+$ which in turn isomerizes to *cis*,*mer*$^+$ to continue the process until all of the *cis*,*fac* is converted to *cis*,*mer*. The same cycle is initiated also after only a single voltammogram, but the process takes longer due to the extremely small amount of oxidized material generated by this kind of experiment.

(iv) Compound D. After elution of compounds **A**−**C** and *cis*,*mer*-$Re(CO)_2(P_2P')Cl$ there were still two ^{31}P NMR resonances in the original mixture which were unaccounted for in the isolated products, suggesting that a further species had been retained on the column. The column was flushed with acetonitrile and then water, but the resonances were still not detected in the ^{31}P NMR spectra of the collected fractions. After allowing the silica to dry, it was soaked in dichloromethane overnight and the solution then filtered. The NMR spectrum of the solution shows the missing resonances at δ 65.7 and 27.6 ppm (1:2), and the IR spectrum shows carbonyl bands at 2040 and 1962 cm^{-1} with the lower frequency band being rather broad. These absorptions are at higher frequencies than others reported in this paper, and the spectral pattern is similar to those for the group 6 metal complexes *fac*-$M(CO)_3(P_2P')$,[11] both of which suggest the compound may be *fac*-$[Re(CO)_3(P_2P')]Cl$. The ES mass spectrum of the solution provides unequivocal proof for the presence of $[Re(CO)_3(P_2P')]^+$ since the intact ion is observed at *m*/*z* 805. As the collision energy is raised from 40 V increasing amounts of fragmentation products are observed (Table 4), but even at a B1 voltage of 180 V the intact ion is still observed, showing that it has extraordinary stability. Thus, the combination of spectroscopic and mass spectral data identifies compound **D** as *fac*-$[Re(CO)_3(P_2P')]Cl$.

I. Description of the Structures of *cis*,*mer*-$Re(CO)_2(P_2P')Cl(I)\cdot CH_2Cl_2$ and *cis*,*mer*-$Re(CO)_2(P_2P')Cl(II)$. The structure of *cis*,*mer*-$Re(CO)_2(P_2P')Cl(I)\cdot CH_2Cl_2$ consists of discrete molecules with one dichloromethane solvate molecule associated with each molecule of the rhenium complex. There are three independent molecules in the asymmetric unit, although their geometries are very similar, giving a total of 12 molecules in the unit cell. Important bond lengths and bond angles are given in Tables 7 and 8. Figure 5 is an ORTEP[24] diagram showing the molecular geometry of *cis*,*mer*-$Re(CO)_2(P_2P')Cl(I)$

(23) Bond, A. M.; Colton, R.; McGregor, K. *Inorg. Chem.* **1986**, *25*, 2378.
(24) Johnson, C. K. *ORTEP II, Fortran Thermal Ellipsoid Plot Program*; Oak Ridge National Laboratory: Oak Ridge, TN, 1976.

Table 7. Interatomic Distances (Å) for *cis,mer*-$Re(CO)_2(P_2P')Cl(I)\cdot CH_2Cl_2$[a]

	molecule 1	molecule 2	molecule 3
Re*−Cl*	2.525 (2)	2.508 (2)	2.513 (2)
Re*−P*1	2.397 (2)	2.424 (2)	2.403 (2)
Re*−P*2	2.420 (3)	2.419 (3)	2.418 (2)
Re*−P*3	2.404 (2)	2.399 (3)	2.413 (2)
Re*−C*11	1.884 (9)	1.867 (8)	1.911 (10)
Re*−C*12	1.931 (10)	1.931 (10)	1.914 (10)
C*11−O*11	1.169 (10)	1.179 (10)	1.151 (12)
C*12−O*12	1.149 (12)	1.141 (13)	1.148 (13)
	Dichloromethane Molecules		
C14−C411	1.733 (20)		
C15−C411	1.679 (20)		
C16−C412	1.646 (17)		
C17−C412	1.791 (20)		
C18−C413	1.586 (21)		
C19−C413	1.552 (18)		

[a] * = 1 for molecule 1; = 2 for molecule 2; = 3 for molecule 3.

Table 8. Interatomic Bond Angles (deg) for *cis,mer*-$Re(CO)_2(P_2P')Cl(I)\cdot CH_2Cl_2$

	molecule 1	molecule 2	molecule 3
Cl*−Re*−P*1	85.58 (8)	82.73 (8)	82.47 (8)
Cl*−Re*−P*2	81.08 (8)	81.13 (8)	81.92 (8)
Cl*−Re*−P*3	83.18 (8)	82.94 (8)	85.71 (8)
Cl*−Re*−C*11	178.3 (4)	176.7 (4)	177.6 (4)
Cl*−Re*−C*12	90.0 (4)	92.8 (4)	92.7 (4)
P*1−Re*−P*2	81.80 (8)	81.00 (8)	81.01 (8)
P*1−Re*−P*3	161.40 (8)	159.10 (8)	160.65 (8)
P*1−Re*−C*11	93.1 (3)	100.5 (4)	99.4 (4)
P*1−Re*−C*12	99.0 (4)	97.3 (4)	95.5 (4)
P*2−Re−P*3	81.85 (8)	81.82 (8)	82.20 (8)
P*2−Re*−C*11	99.8 (4)	98.7 (4)	96.9 (4)
P*2−Re*−C*12	171.0 (4)	173.8 (4)	173.9 (4)
P*3−Re*−C*11	98.4 (4)	93.8 (4)	92.1 (4)
P*3−Re*−C*12	95.8 (4)	98.5 (4)	100.4 (4)
C*11−Re*−C*12	89.1 (4)	87.4 (5)	88.5 (5)
Re*−C*11−O*11	177.5 (7)	176.0 (7)	174.3 (7)
Re*−C*12−O*12	179.0 (7)	176.8 (8)	177.6 (8)
	Dichloromethane Molecule Angles		
C14−C411−C15	120.9 (10)		
C16−C412−C17	105.1 (10)		
C18−C413−C19	128.0 (16)		

[a] * = 1 for molecule 1; = 2 for molecule 2; = 3 for molecule 3.

(molecule 1), together with the atomic numbering scheme. The hydrogen atoms are not labeled but carry the same number as the carbon atom to which they are attached. The octahedral coordination of the rhenium atom is derived from the two carbonyl groups which are mutually *cis*, the three phosphorus atoms of P_2P' which adopt a *mer* stereochemistry, and the chlorine atom.

The structure of *cis,mer*-$Re(CO)_2(P_2P')Cl(II)$ also consists of discrete molecules of the rhenium complex, but no solvate is incorporated into this structure. There is only one rhenium molecule is the asymmetric unit, giving four molecules in the unit cell. Important bond lengths and bond angles are given in Tables 9 and 10. Figure 6 is an ORTEP diagram showing the molecular geometry of *cis,mer*-$Re(CO)_2(P_2P')Cl(II)$. The stereochemical arrangement of ligands about the rhenium is very similar to that in *cis,mer*-$Re(CO)_2(P_2P')Cl(I)$, but the differences lie in the spatial relationships between the coordinated ligands and the phenyl rings of P_2P'. The *mer* configuration of P_2P' forces an arrangement of the phenyl rings such that three of them (one from each P, the other from P′) are on one side of the rhenium atom, and they form a cavity enclosing one of the ligands coordinated to rhenium. The other two phenyl groups are on the other side of the rhenium atom where there is a much more open environment. One carbonyl group and the chlorine

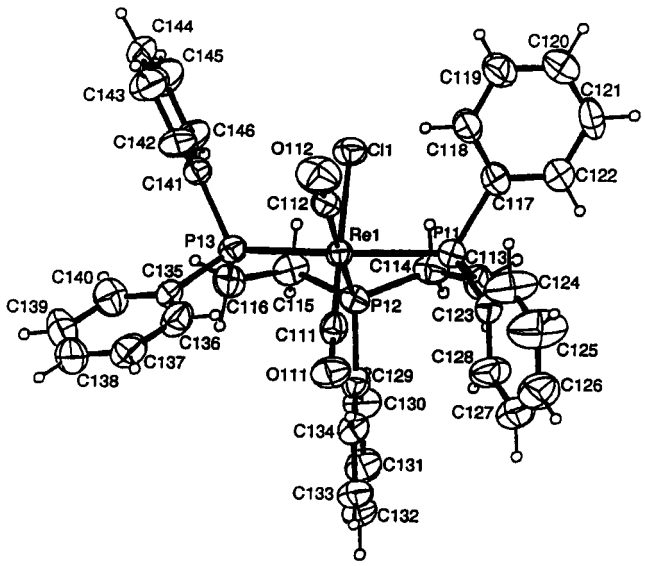

Figure 5. ORTEP diagram of *cis,mer*-$Re(CO)_2(P_2P')Cl(I)\cdot CH_2Cl$ (molecule 1) with ellipsoids scaled to 40% probability. The CH_2Cl_2 molecules and hydrogen atoms have been omitted for clarity.

Table 9. Interatomic Distances (Å) for *cis,mer*-$Re(CO)_2(P_2P')Cl(II)$

Re−Cl	2.506 (1)	Re−P1	2.411 (1)
Re−P2	2.412 (1)	Re−P3	2.395 (1)
Re−C1	1.892 (3)	Re−C2	1.933 (3)
C1−O1	1.153 (4)	C2−O2	1.154 (4)

Table 10. Interatomic Bond Angles (deg) for *cis,mer*-$Re(CO)_2(P_2P')Cl(II)$

Cl−Re−P1	89.87 (3)	Cl−Re−P2	93.99 (3)
Cl−Re−P3	97.62 (3)	Cl−Re−C1	178.4 (1)
Cl−Re−C2	87.2 (1)	P1−Re−P2	81.89 (3)
P1−Re−P3	162.96 (3)	P1−Re−C1	88.5 (1)
P1−Re−C2	98.3 (1)	P2−Re−P3	82.34 (3)
P2−Re−C1	85.7 (1)	P2−Re−C2	178.8 (1)
P3−Re−C1	83.9 (1)	P3−Re−C2	97.3 (1)
C1−Re−C2	93.1 (1)	Re−C1−O1	178.0 (3)
Re−C2−O2	178.2 (3)		

ligand are mutually *trans* to each other in the overall *cis,mer* stereochemistry. In structure (I) this carbonyl is enclosed in the cavity while in structure (II) it is the chlorine which is inside the cavity.

The Re−P bond lengths are similar and agree with values from previous structure determinations, as do the Re−Cl and Re−C bond lengths.[25−31] The nature of the ligand *trans* to the metal−CO and metal−P bonds is known to influence these bond distances. The Re−C bond of a carbonyl ligand *trans* to a phosphorus is expected to be longer than Re−C bonds in which the carbonyl is *trans* to a chlorine atom, since phosphorus has some π-bonding ability, but the metal−halogen bond is regarded as predominantly σ in nature. This characteristic behavior is exhibited by both rhenium complexes, where the Re−C bond *trans* to a phosphorus atom is observed to be approximately

(25) Davis, B. R.; Ibers, J. A. *Inorg. Chem.* **1971**, *10*, 578.
(26) Albano, V. G.; Bellon, P. L.; Cianai, G. *J. Organomet. Chem.* **1971**, *31*, 75.
(27) Anglin, J. R.; Calhoun, H. P.; Graham, W. A. G. *Inorg. Chem.* **1977**, *16*, 2281.
(28) Rossi, R.; Duatti, A.; Magon, L.; Cassellato, U.; Graziani, R.; Toniolo, L. *Inorg. Chim. Acta* **1983**, *75*, 77.
(29) Lin, S. C.; Cheng, C. P.; Lee, T.-Y.; Lee, T.-J.; Peng, S. M. *Acta Crystallogr.* **1986**, *C42*, 1733.
(30) Rossi, R.; Marchi, A.; Duatti, A.; Magon, L.; Cassellato, U.; Graziani, R. *J. Chem. Soc., Dalton Trans.* **1987**, 2299.
(31) Lui, L.-K.; Lin, S. C.; Cheng, C. P. *Acta Crystallogr.* **1988**, *C44*, 1402.

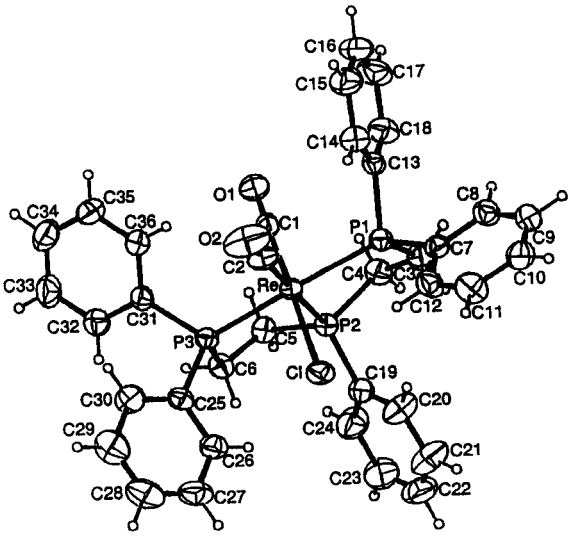

Figure 6. ORTEP diagram of *cis,mer*-$Re(CO)_2(P_2P')Cl$(II) with ellipsoids scaled to 40% probability. The hydrogen atoms have been omitted for clarity.

0.04 Å longer than the Re−C bond *trans* to the chlorine. The Re−P bond lengths are as expected shorter when these bonds involve *trans* phosphorus atoms than the Re−P bonds in which the phosphorus atom is *trans* to a carbonyl group, as the carbonyl group is a strong π-acceptor. For these two rhenium complexes there is only a marginal difference in these bond lengths. In structure (I) the average Re−P distance involving the phosphorus *trans* to a carbonyl group is 2.419 (3) Å, while the average of the mutually *trans* Re−P bond lengths are 2.405 (2) and 2.408 (2) Å. For structure (II) the corresponding values are 2.412 (1) Å compared with 2.395 (1) and 2.411 (1) Å.

The geometry of the ligands about rhenium shows a distorted octahedral coordination in both structures, with structure (I) showing the greater degree of distortion. The two P−Re−P bite angles are significantly less than 90° for both structures (average angles are 81.27 (8) and 81.96 (8)° for (I) and 81.93 (3) and 82.34 (3)° for (II)), obviously due to the strain about the central phosphorus atom when P_2P' chelates in the *mer* configuration to form two five-membered rings. Therefore, P(*1) and P(*3) are tilted slightly towards P(*2) (* = 1, 2, or 3 for molecules 1, 2, or 3). The P(*2)−Re(*)−C(*11) angle in structure (I) has an average value of 97.7 (4)°, while the corresponding angle for structure (II) is 85.7 (1)°. The average Cl(*)−Re(*)−P(*2) angle of structure (I) is 82.9 (7)°, while the analogous angle for structure (II) is 93.8 (3)°, which is closer to the idealized value for octahedral geometry. Thus, in *cis,mer*-$Re(CO)_2(P_2P')Cl$(I) the chlorine atom is tilted toward P(*2), whereas in *cis,mer*-$Re(CO)_2(P_2P')Cl$(II) the chlorine atom points slightly away from P2. The Re−C−O angles range from 174.3 (7) to 179.0 (7)° and are comparable to values obtained for other rhenium carbonyl complexes.

Each phenyl ring of the two complexes is planar to within experimental errors. The plane equations and deviations are given in the Supporting Information. In structure (II), the rhenium atom is located very close to the plane defined by P_3C; its deviation from the plane is 0.08 Å, while the other atoms are coplanar to within 0.06 Å. However for structure (I), the rhenium atom lies slightly further from the plane defined by P_3C, occurring at 0.19 Å from the plane for molecule 1 (other atoms coplanar to within 0.02 Å), 0.19 Å from the plane for molecule 2 (others coplanar to within 0.08 Å), and 0.08 Å from the plane for molecule 3 (others coplanar to within 0.06 Å). An examination of all possible intermolecular contacts did not reveal any unusual features.

Conclusions and General Discussion

The product of the reaction between $Mn(CO)_5X$ and P_2P' was formulated as *cis,mer*-$Mn(CO)_2(P_2P')X$ on the basis of spectroscopic evidence. However, the results from the corresponding rhenium system show that two forms of the *cis,mer* geometry are possible, depending on the orientation of the different *trans* ligands to the cavity generated by the P_2P' ligand. There is no direct spectroscopic evidence to distinguish which isomer is present for manganese, but all measurements indicate only one *cis,mer* isomer is present. The close similarity of the complex electrochemical behaviors of *cis,mer*-$Mn(CO)_2(P_2P')X$ and *cis,mer*-$Re(CO)_2(P_2P')X$(I) on the voltammetric time scale implies they are the same isomer. The strongest evidence for this lies in the presence of the redox couple 4,4′ for all these compounds, but its absence, for the *cis,mer*-(II) isomer of the rhenium compounds. The full significance of the absence of processes 4,4′ for the *cis,mer*-(II) isomers will be discussed below. It will be assumed, however, that the manganese complexes are *cis,mer*-(I). No evidence was found for the *cis,fac*-(I) isomer (Figure 1) with any compound. Presumably, steric interaction between the halogen and a phenyl ring on the adjacent phosphorus atom is sufficient to destabilize this isomer in favor of *cis,fac*-(II). A simple rotation of the CO,CO,X face of the octahedron in either the 17- or 18-electron state would interconvert these isomers.

It is well-known that when 18-electron *cis*-dicarbonyl and *fac*-tricarbonyl complexes are oxidized to the 17-electron state, there is a tendency for them to isomerize rapidly to the *trans*- and *mer*-carbonyl stereochemistries. Numerous examples have been described,[32] and a theoretical justification for the process has been presented.[33]

Previous studies have shown that in the $[M(CO)_3(P_2P')]^{+/0}$ (M = Mo, W) system there is very rapid isomerization between *fac* and *mer* geometries in both the 17- and 18-electron configurations,[11] which was assumed to proceed via an internal twist mechanism. This behavior was attributed to stereochemical strain in both geometries, so that neither form is particularly favorable. In the *fac* geometry there is steric interaction between two phenyl rings, one from each terminal phosphorus, and in the *mer* geometry there is angular strain associated with the central phosphorus of P_2P'.

The behavior of the oxidation products of *cis,mer*-$Mn(CO)_2(P_2P')X$ and *cis,mer*-$Re(CO)_2(P_2P')X$(I) show features of both these characteristic patterns. The isomerization of *cis,mer*$^+$ to *trans*$^+$, which is carbonyl controlled, is slower than usual on the voltammetric time scale, although the reaction does proceed to completion on the longer time scale. Since this carbonyl isomerization is slow on the voltammetric time scale, it allows another isomerization to *cis,fac*$^+$ to be observed, and this process is controlled by the P_2P' ligand. Unlike the *cis,mer*$^+ \rightarrow$ *trans*$^+$ isomerization, which, although slow, is essentially one-way, there is a fast isomerization between *cis,mer*$^+$ and *cis,fac*$^+$ as evidenced by the behavior of processes 1,1′ and 4,4′ as a function of temperature. In contrast, *cis,mer*-$Re(CO)_2(P_2P')X$(II) gives no evidence for any isomerization to a *cis,fac* isomer in either the 17- or 18-electron state under voltammetric conditions, so it seems likely that the presence of the larger halo ligand within the cavity of phenyl rings prevents the operation on the twist mechanisms which interconvert the isomers. It is this phenomenon which allows both *cis,mer* isomers of $Re(CO)_2(P_2P')X$ to be isolated, since their interconversion must proceed

(32) (a) Geiger, W. E. *Prog. Inorg. Chem.* **1985**, *33*, 275. (b) Bond, A. M.; Colton, R.; McCormick, M. J. *Inorg. Chem.* **1977**, *16*, 155. (c) Bond, A. M.; Colton, R.; Jackowski, J. J. *Inorg. Chem.* **1975**, *14*, 274.
(33) Mingos, D. M. P. *J. Organomet. Chem.* **1979**, *179*, C29.

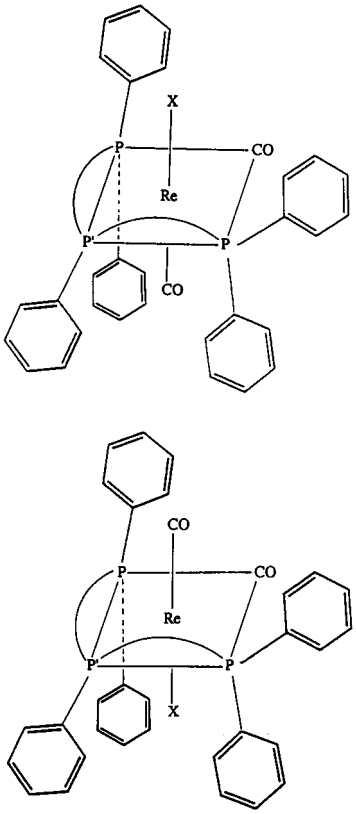

Figure 7. Diagrammatic representations of the two isomers of *cis,mer*-$Re(CO)_2(P_2P')Cl$.

via the *fac* isomer, if a twist mechanism is operative. The following scheme can therefore be justified

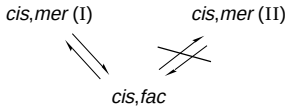

(12)

However, these isomerizations do proceed at high temperatures in refluxing mesitylene on the longer time scale since short reflux times give a mixture of isomers of $Re(CO)_2(P_2P')Cl$, but longer reaction times (24 h) give only *cis,mer*-$Re(CO)_2(P_2P')Cl$(I).

Diagrammatic representation of the two isomers of *cis,mer*-$Re(CO)_2(P_2P')Cl$ are shown in Figure 7. Several conditions are necessary to observe this type of isomerism and all must be operative. (i) When coordinated, the polydentate ligand must generate an unsymmetric environment on two sides of the metal. (ii) None of the ligands can be labile, otherwise fluxional coordinatively unsaturated intermediates would be formed which would allow rapid interconversion of the isomers. (iii) There must be two different groups in the *trans* positions, at least one of which must be large enough to sterically block internal twist mechanisms which would lead to isomerization. In *cis,mer*-$Re(CO)_2(P_2P')Cl$ the halo ligand fulfills this requirement, although the carbonyl group does allow twist mechanisms to occur as evidenced by the $M(CO)_3(P_2P')$ systems and the *cis,mer*-$Re(CO)_2(P_2P')Cl$(I) $\rightleftharpoons$ *cis,fac*-$Re(CO)_2(P_2P')Cl$ isomerization.

Acknowledgment. We thank Dr. Alison Edwards, School of Chemistry, University of Melbourne, for arranging for the collection of crystallographic data. We thank Assoc. Prof. F. R. Keene, James Cook University, Townsville, Australia, and Prof. A. von Zelewsky, University of Fribourg, Switzerland, for helpful comments on the isomerism of *cis,mer*-(I) and *cis,mer*-(II). J.N.W. thanks the Commonwealth Government of Australia for a Post Graduate Research Award. The financial support of the Australian Research Council is gratefully acknowledged.

Supporting Information Available: Tables S-1−S-24 listing positional parameters, anisotropic thermal parameters, hydrogen coordinates, interatomic distances in the phenyl rings, least squares planes, deviations from least squares planes, dihedral angles between least squares planes, and intermolecular contacts less than 3.5 Å for both structures, and figures showing packing diagrams for both structures (48 pages). This material is contained in many libraries on microfiche, immediately follows this article in the microfiche version of the journal, can be ordered from the ACS, and can be downloaded from the Internet; see any current masthead page for ordering information and Internet access instructions.

IC961295D